Applied Problems of Nonlinear Oscillation and Wave Theory

Izvestiya Vysshikh Uchebnykh Zavedeniy. Applied Nonlinear Dynamics. 2023;31(3)

Article DOI: 10.18500/0869-6632-003041

Application of joint singularity spectrum to analyze cooperative dynamics of complex systems

G. A. Guyo, A. N. Pavlov✉

Saratov State University, Russia
E-mail: guyo199814@gmail.com, ✉pavlov.alexeyn@gmail.com

Received 23.01.2023, accepted 4.04.2023, available online 21.04.2023, published 31.05.2023

Abstract. *Purpose* of this work is to generalize the wavelet-transform modulus maxima method to the case of cooperative dynamics of interacting systems and to introduce the joint singularity spectrum into consideration. The research *method* is the wavelet-based multifractal formalism, the generalized version of which is used to quantitatively describe the effect of chaotic synchronization in the dynamics of model systems. Models of coupled Rössler systems and paired nephrons are considered. As a *result* of the studies carried out, the main changes in the joint singularity spectra were noted during the transition from synchronous to asynchronous oscillations in the first model and to the partial synchronization mode in the second model. *Conclusion.* Proposed approach can be used in studies of the cooperative dynamics of systems of various nature.

Keywords: multifractal formalism, joint singularity spectrum, synchronization of oscillations, wavelet transform.

Acknowledgements. This work was supported by Russian Science Foundation, project No. 22-22-00065.

For citation: Guyo GA, Pavlov AN. Application of joint singularity spectrum to analyze cooperative dynamics of complex systems. Izvestiya VUZ. Applied Nonlinear Dynamics. 2023;31(3):305–315. DOI: 10.18500/0869-6632-003041

Introduction

Complex systems often include interacting components that can exhibit complex behavior. A change in the dynamics of such systems is a consequence of a change in the functioning of individual components or the connections between them. In the latter case, it is important to obtain information about the cooperative dynamics of elements of a complex system (for example, a complex network) using quantitative criteria that reflect the interaction of subsystems. For this purpose, cross-spectra, cross covariation or correlation functions [1], as well as special characteristics (for example, measures of mutual information [2]) can be used. The dynamics of individual elements can demonstrate a multifractal structure. For its quantitative description, a single value reflecting the features of the frequency dependence of the spectral power density or the decay of correlations is not enough. When conducting research, an approach based on

the calculation of the singularity spectrum [3] is often used. Many methods of calculating this spectrum are known. Each method has its own possibilities and limitations. For example, the approach based on structure functions [4, 5] is not suitable for studying weak singularities. Multifractal formalism based on wavelets [6, 7] and multifractal fluctuation analysis [8, 9] are considered more universal methods. The multifractal formalism, due to the choice of a suitable wavelet function (having a large number of vanishing moments), makes it possible to ignore the polynomial trend in experimental data. Generalization of the concept of multifractals to the case of cooperative dynamics of complex systems was proposed in [10], where joint multifractal measures were introduced. However, the article [10] was based on the classical approach to analysis, which provides for covering a fractal set with geometric objects (for example, cubes), which has a number of limitations when studying signals.

In this paper, we consider a generalization to the case of joint dynamics of systems with self-sustained oscillations of the wavelet-transform modulus-maxima method, in which wavelet functions are selected as elements of the coverage. This makes it possible to use a more universal approach applicable both to stationary processes and to signals of systems with time-varying characteristics. At the same time, the analysis of both strong and weak singularities (large and small fluctuations) is provided using the algorithm for calculating generalized partition functions. We illustrate the proposed generalized method by the example of the effect of synchronization of chaotic oscillations in model systems: a model of two coupled Rössler systems and a more complex model of paired nephrons.

1. Methods

1.1. Method for calculating the joint singularity spectrum. A multifractal formalism based on wavelets was proposed in [6] and tested on various examples in subsequent publications [7, 11–13]. It provides for the calculation of the maxima of the modules (skeleton) of the wavelet transform, which contains basic information about the signal, and the analysis of the power laws of the wavelet coefficients depending on the scale [14]. Algorithmic calculations of the singularity spectrum of the function $f(t)$ can be divided into two stages, the first of which is the calculation of the coefficients of the continuous wavelet transform

$$W(a,b) = \frac{1}{a}\int_{-\infty}^{\infty} f(t)\psi\left(\frac{t-b}{a}\right)dt, \tag{1}$$

where a is the scale parameter, b characterizes the translation of the wavelet function ψ, and the distribution function of the analyzed signal is considered as $f(t)$. The choice of the basic function ψ is determined by the specifics of the analyzed process. Theoretically, the singularity spectrum does not depend on the choice of a basis. But in the case of non-stationary processes, the presence of a trend has an impact on the estimates being made. In problems of multifractal analysis, wavelet bases constructed on the basis of derivatives of the Gaussian function are often used

$$\psi^{(m)} = (-1)^m \frac{\partial^m}{\partial t^m}\left[\exp\left(-\frac{t^2}{2}\right)\right], \tag{2}$$

for example, WAVE ($m = 1$) or MHAT ($m = 2$). In this paper, we used the MHAT-wavelet.

The researcher needs to assess the sensitivity of the results to the choice of algorithmic parameters, in particular, the range of scales for studying and quantifying the properties of fractality.

If there is a singular behavior at a point t^*, in the neighborhood of this point $f(t)$ can be represented as

$$f(t) = P_n(t) + C|t - t^*|^{h(t^*)}, \tag{3}$$

that is, in the form of a regular component $P_n(t)$ (a polynomial of degree n) and a term describing a singularity, which is characterized by a non-integer value $h(t^*)$. When choosing a wavelet having m zero moments ($m \geqslant n$),

$$\int_{-\infty}^{\infty} P_n(t)\psi(t)dt = 0, \tag{4}$$

as a result of the wavelet analysis, we get a power dependence

$$W(a, t^*) \sim a^{h(t^*)}. \tag{5}$$

This power dependence is quantitatively described by the Hölder exponent $h(t^*)$. Each singularity leads to the appearance of one or more lines of local maxima of the wavelet transform modules (skeleton lines). Therefore, all the information about the singularities of $f(t)$ is contained in the skeleton of the wavelet transform.

However, it is difficult to perform calculations using the formula (5) due to the influence of neighboring singularities that prevent consideration of an acceptable scale range for calculations. For this reason, as the second stage of calculations in [7], it is proposed to construct generalized partition functions

$$Z(q, a) = \sum_{l \in L(a)} \left(\sup_{\acute{a} \leqslant a} | W(\acute{a}, b_l(\acute{a})) | \right)^q, \tag{6}$$

where $L(a)$ — a complete set of local extremum lines $W(a, b)$ on the scale a, $b_l(\acute{a})$ — location on the scale $\acute{a} \leqslant a$ of the maximum, which refers to the line l, and sup is considered in order to avoid the appearance of zero values for negative q. According to the conclusions of [6, 7], generalized partition functions usually exhibit power-law behavior

$$Z(q, a) \sim a^{\tau(q)}, \tag{7}$$

where $\tau(q)$ are the scaling exponents, which are intermediate values in the calculation of the Hölder exponents $h(q)$ and the singularity spectrum $D(h)$

$$D(h) = qh - \tau(q), \quad h(q) = \frac{d\tau(q)}{dq}. \tag{8}$$

The description of the algorithm of the wavelet-transform modulus-maxima is given in more detail in [7]. The calculation of $\tau(q)$ is carried out by linear segments of the dependencies $\lg Z(q, a)$ from $\lg a$ (we used the range $\lg a \in [0.7, 4.0]$).

Let's consider a generalization of this algorithm for the case of cooperative dynamics of complex systems - to describe complex scaling in the functioning of interacting subsystems by signals reflecting the functioning of each of them. Let $f(t)$ and $g(t)$ be the distribution functions of the two analyzed processes. We calculate a continuous wavelet transform for each of them

$$\begin{aligned} W_f(a, b) &= \frac{1}{a} \int_{-\infty}^{\infty} f(t)\psi\left(\frac{t-b}{a}\right) dt, \\ W_g(a, b) &= \frac{1}{a} \int_{-\infty}^{\infty} g(t)\psi\left(\frac{t-b}{a}\right) dt \end{aligned} \tag{9}$$

and the corresponding skeletons. There are several possible solutions to the problem of joint multifractal analysis. For example, we can initially consider the mutual wavelet transform of

distribution functions with the allocation of its modulus-maxima. In this paper, we have chosen a relatively simple approach consisting in modifying the procedure for calculating generalized partition functions

$$Z^2(q,a) = \sum_{i\in L_f(a)} \left(\sup_{\acute{a}\leqslant a} \mid W_f(\acute{a}, b_i(\acute{a})) \mid \right)^q \times \sum_{j\in L_g(a)} \left(\sup_{\tilde{a}\leqslant a} \mid W_g(\tilde{a}, b_j(\tilde{a})) \mid \right)^q. \qquad (10)$$

Here $L_f(a)$ and $L_g(a)$ denote the skeletons for each of the distribution functions, $b_i(\acute{a})$ and $b_j(\tilde{a})$ — location on the scales $\acute{a} \leqslant a$ and $\tilde{a} \leqslant a$ of maxima that relate to the lines i and j. Further calculations are carried out in accordance with the previously given algorithm, that is, scaling exponents $\tau(q)$ and the singularity spectrum $D(h)$ are calculated according to the formulas (7) and (8). All parameters of the algorithm are chosen the same as for calculations based on a single signal. However, now the calculated singularity spectrum can be interpreted as a joint one, since it reflects the joint dynamics of the subsystems generating the analyzed signals. To test the proposed approach, consider two examples of mathematical models.

1.2. Coupled Rössler Systems. Rössler's model of two coupled systems is often used as a basic example for testing various signal analysis methods. Its dynamics is well studied, and the presence of various variants of complex oscillations in this model makes it possible to analyze the possibility of diagnosing the change of operating modes when the control parameters change. The model is described by the following system of ordinary differential equations of the 1st order:

$$\begin{aligned} \frac{dx_{1,2}}{dt} &= -\omega_{1,2}y_{1,2} - z_{1,2} + \gamma(x_{2,1} - x_{1,2}), \\ \frac{dy_{1,2}}{dt} &= \omega_{1,2}x_{1,2} + ay_{1,2}, \\ \frac{dz_{1,2}}{dt} &= b + z_{1,2}(x_{1,2} - c), \end{aligned} \qquad (11)$$

parameters $a = 0.15$, $b = 0.2$ and c determine the dynamics mode of individual subsystems, and $\gamma = 0.02$ is the coupling strength. To consider non-identical subsystems, we introduce frequency detuning $\omega_{1,2} = 1.0 \pm \Delta$, and select two control parameters c and Δ, the variation of which allows us to observe modes of synchronous and non-synchronous chaotic oscillations, hyperchaotic mode, as well as various variants of periodic and quasi-periodic oscillations. In order to study the transverse structure of chaotic attractors, which demonstrates the property of multifractality, it is possible to choose sequences of return times to the Poincaré section as the studied signals.

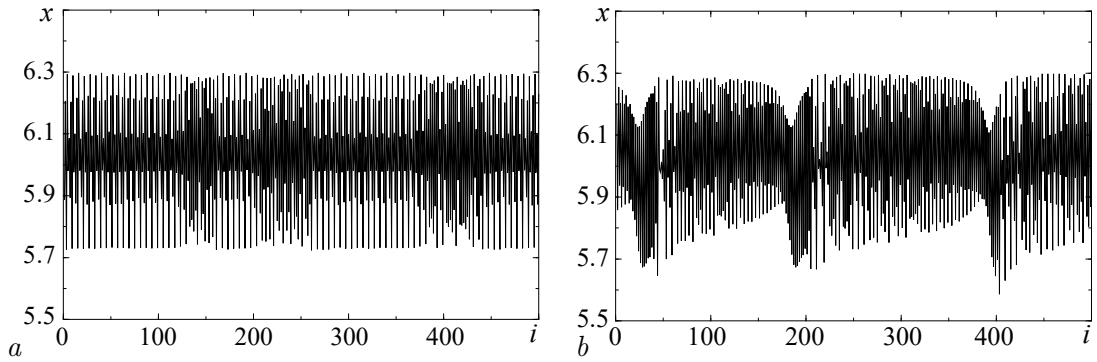

Fig. 1. Return time sequences into the Poincaré section $x_1 = 0$ for synchronous (a) and asynchronous (b) chaos in the model of two coupled Rössler systems

Consider as analyzed signals sequences of return times to the secant planes $x_1 = 0$ and $x_2 = 0$ corresponding to the modes of synchronous chaos ($c = 6.8$, $\Delta = 0.009$) and non-synchronous chaos ($c = 6.8$, $\Delta = 0.010$). In Fig. 1 the sequences of return times to the Poincaré section $x_1 = 0$ for the selected modes are given. They are visually different, so we can expect significant differences in the characteristics of the multifractal structure of the corresponding attractors.

1.3. Model of paired nephrons. The model of paired nephrons is more complex. For one structural element of the kidney, it was proposed in [15] and constructed in accordance with physiological concepts of renal autoregulation of blood flow. The model turned out to be successful because it allows us to describe many features of the real dynamics of nephrons that have been found in numerous experimental studies. For example, the model well describes the transition from almost regular oscillations in fluid pressure in the proximal tubules of nephrons (the case of the norm) to highly irregular in renal hypertension. The model is very complex, and its full description takes several pages. For this reason, in this article we give only a schematic description

$$\begin{aligned}
\frac{dP_t}{dt} &= \frac{1}{C_{\text{tub}}}\left\{F_f\left(P_t, r\right) - F_{\text{reab}} - \left(P_t - P_d\right)/R_{\text{Hen}}\right\},\\
\frac{dr}{dt} &= v_r,\\
\frac{dv_r}{dt} &= \frac{1}{\omega}\left\{P_{av}\left(P_t, r\right) - P_{eq}\left(r, \Psi(X_3, \beta)\right) - \omega d v_r\right\},\\
\frac{dX_1}{dt} &= \frac{1}{R_{\text{Hen}}}\left(P_t - P_d\right) - \frac{3}{T}X_1,\\
\frac{dX_2}{dt} &= \frac{3}{T}\left(X_1 - X_2\right),\\
\frac{dX_3}{dt} &= \frac{3}{T}\left(X_2 - X_3\right).
\end{aligned} \tag{12}$$

The variable P_t describes the pressure in the proximal tubule, F_f — glomerular filtration rate, C_{tub} — elastic conductance of the tubule. The difference $P_t - P_d$ between the proximal and distal pressure and the resistance R_{Hen} determine the fluid flow in the Henle loop. Reabsorption in the proximal tubule F_{real} is considered a constant value. The second and third equations characterize the dynamics caused by the control of the flow in the afferent arteriole. Here r is the radius of the vessel, v_r is the rate of its change, d describes the damping of oscillations, ω is a measure of mass relative to the elastic conductance of the arteriole wall, P_{av} denotes the average pressure in the arteriole. P_{eq} represents the value of this pressure at which the arteriole is in equilibrium with its current radius value and muscle activation Ψ. The expressions for F_f, P_{av} and P_{eq} include a number of algebraic equations that must be solved together with the integration of the (12) system. The three remaining equations describe the delay T in the mechanism of tubulo-glomerular feedback, which is the cause of the appearance of slow oscillations of the variable P_t with a frequency of 0.02...0.04 Hz. The myogenic mechanism described by the second and third equations leads to faster oscillations (0.1...0.2 Hz). Their amplitude is much smaller than the amplitude of a slow rhythm. The transition from normal blood pressure to renal hypertension is accompanied by an increase in the feedback strength (parameter β of the model (12)). An example of the chaotic dynamics of the (12) model is shown in Fig. 2.

The interaction of paired nephrons is determined by electrochemical signals. In the model (12), the equilibrium pressure in the afferent arteriole depends on the current radius r and the activation level Ψ of smooth muscles. Muscle activation spreads along the afferent arteriole in a damped manner. When it reaches the branching point with the arteriole of the neighboring

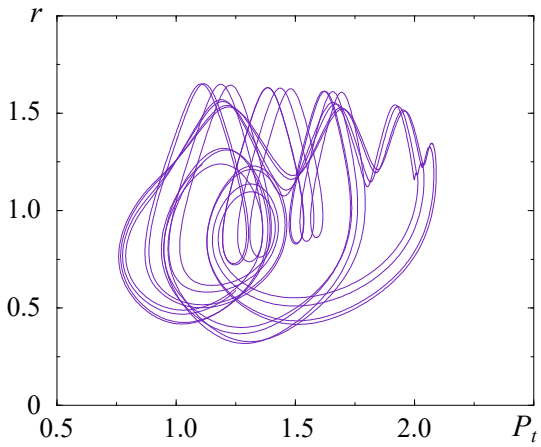

Fig. 2. An example of chaotic oscillations in nephron model

nephron, part of the signal can propagate along it and affect the neighboring nephron. In the paired nephron model, this relationship can be described by adding the contribution of the activation level in one nephron to the activation level in the neighboring nephron [16]

$$\Psi^*_{1,2} = \Psi_{1,2} + \gamma\Psi_{2,1}, \tag{13}$$

where γ is the coupling parameter and $\Psi_{1,2}$ is the activation levels of two uncoupled nephrons determined by their respective Henle flows. To separate slow and fast oscillations and characterize them separately, we chose the parameters $\gamma = 0.005$ and $\beta = 27.3$ and considered the sequences of return times in the Poincare section $P_t = 1.6$ and $v_r = 0$. To illustrate the method, let us consider examples of complete synchronization of chaotic oscillations ($T_1 = T_2 = 13.5$ s, where T_1 and T_2 are the delay values in the feedback mechanism for each nephron) and partial chaotic synchronization observed only for slow dynamics ($T_1 = 13.5$ s, $T_2 = 13.4$ s). The analyzed sequences of return times for the selected dynamics modes are shown in Fig. 3.

2. Results

2.1. Coupled Rössler Systems. The transition across the boundary of the chaotic synchronization region in the (11) model is accompanied by significant changes in the joint singularity spectrum. These changes are similar to the previously discussed results for the wavelet-transform modulus-maxima method applied to the analysis of the dynamics of one of the interacting subsystems [12]. However, in this case, the difference lies in considering the spectrum of singularities, which reflects the corporate dynamics of the (11) model. There are two main differences between synchronous and asynchronous modes: a different position of $D(h)$ along the h axis, which can be described by the location of the maximum of the $D(h)$ function, as well as a change in the width of the spectrum — range of Hölder exponents. From the point of view of the first difference, we can state the transition from positively correlated sequences of return times ($h > 0.5$) of the non-synchronous mode to anticorrelated ($h < 0.5$) during synchronization.

Fig. 4 demonstrates a decrease in the average value of the Hölder exponents (corresponding to $q = 0$, that is, the maximum of the singularity spectrum) from 1.16 for non-synchronous chaotic oscillations to 0.01 for synchronous chaos. The second difference is no less clear: the width of the singularity spectrum, which can be interpreted as a measure of the heterogeneity (complexity) of the dynamics mode, decreases from 0.48 to 0.02 when moving into the synchronization region. Thus, it is possible to diagnose the synchronization effect using any of these measures — the

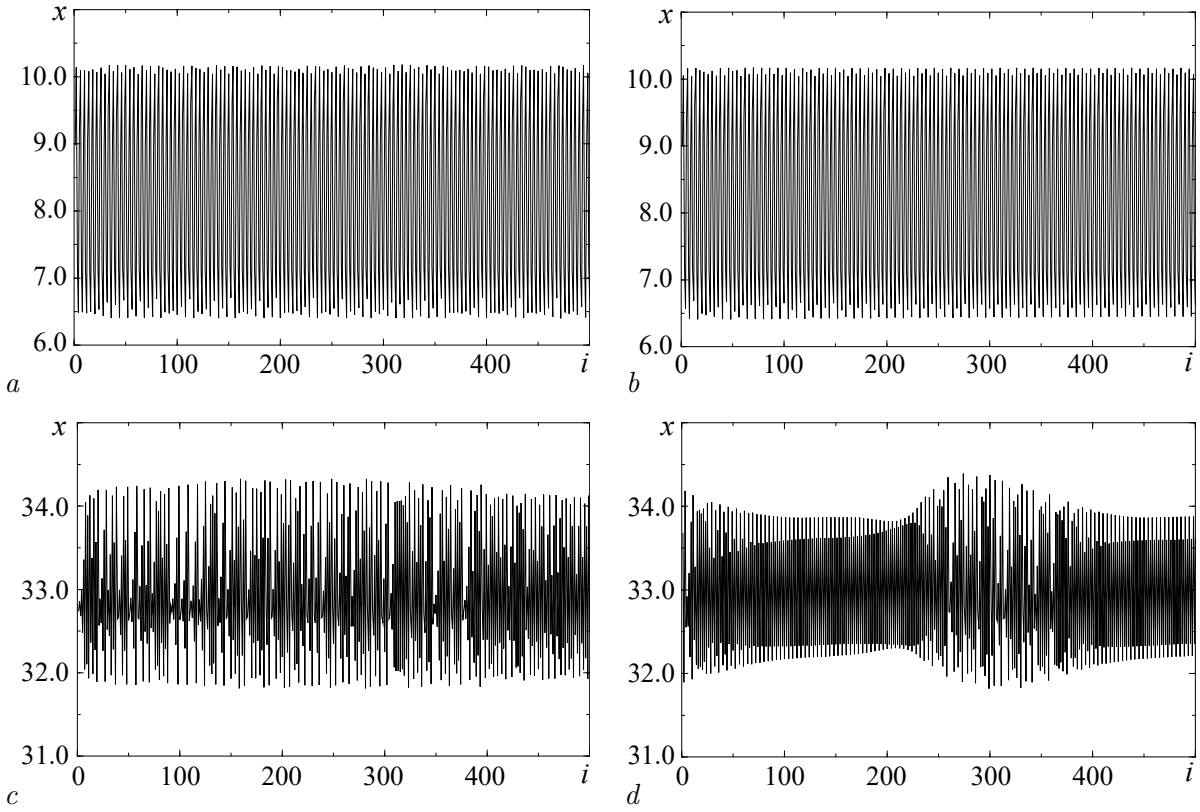

Fig. 3. Return times sequences for fast (*a, b*) and slow (*c, d*) dynamics in the regimes of full synchronization (*a, c*) and partial synchronization (*b, d*) in the model of two paired nephrons (for the first unit)

average value of the Hölder exponents describing the change in the correlation properties of the sequences of return times, or a measure of heterogeneity indicating a decrease in the complexity of the synchronous mode. In this context, complexity is estimated by the number of characteristics that can be used to describe the mode, and not by its predictability.

For example, white noise, which is a delta-correlated process, can be interpreted as simple, since it is described by a single value of the Hölder exponent $h = 0.5$ and a singularity spectrum consisting of a single point. For the example shown in Fig. 4, synchronous mode is also much simpler compared to non-synchronous, although in both cases we are talking about chaotic

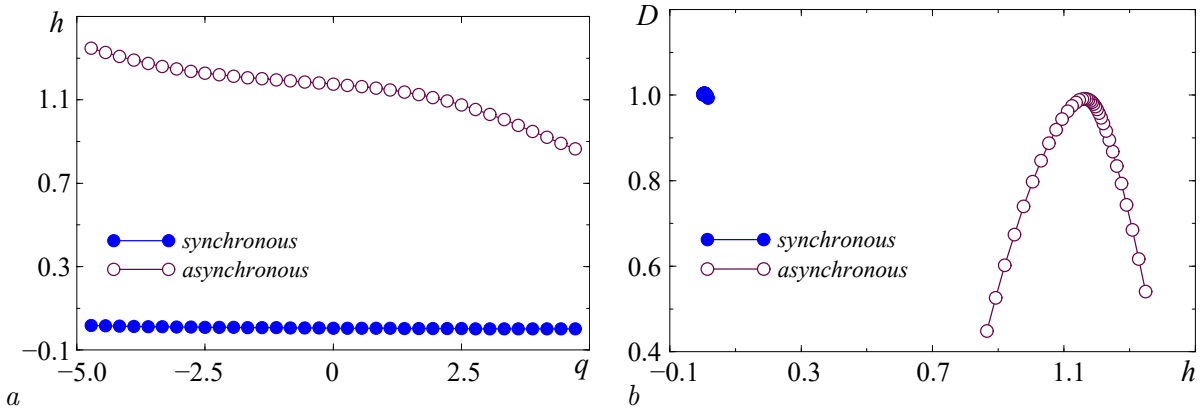

Fig. 4. Multifractal analysis of synchronous and asynchronous dynamics of coupled Rössler systems: *a* — Hölder exponents, *b* — singularity spectra

oscillations in the (11) model. The revealed differences are predictable, taking into account the differences in the sequences of the return times of the modes under consideration (see Fig. 1).

2.2. Model of paired nephrons. With the selected values of the control parameters of the model, (12) demonstrates significantly different behavior for fast and slow rhythms of the structural elements of the kidney (Fig. 5). As noted in [16, 17], for paired nephrons (both in the model and in physiological experiments conducted on laboratory animals), various modes of full, partial synchronization, as well as non-synchronous behavior can be observed. For example, partial synchronization consists in tuning the frequencies of some rhythms in the absence of tuning the frequencies of others. In the example shown in Fig. 5, at $T_2 = 13.4$ s, synchronous dynamics of fast rhythms is observed, accompanied by non-synchronous behavior for slow ones (Fig. 3). This leads to the absence of fundamental differences in the joint singularity spectra for fast rhythmic processes (at $T_2 = 13.4$ s and $T_2 = 13.5$ s, they correspond to the singularity spectra of processes close to monofractal, and the dynamics of fast rhythms is close to periodic).

At the same time, there are differences for the slow dynamics of paired nephrons, and they are significant. Compared to the simpler example of coupled Rössler systems, changes in the joint singularity spectrum are described by one characteristic - the position of the spectrum, that is, the average value of the Hölder exponents. There is a clearly detected transition from positively correlated sequences of return times to the Poincaré section to anticorrelated sequences, and the average value of h decreases from 0.71 to 0.15. The detected change in the type of correlations is a reflection of the coordinated dynamics of subsystems during synchronization. It is quite typical when the connection between subsystems increases or frequency detuning decreases, leading to a transition inside the synchronization area [12]. At the same time, there is no decrease in the width of the joint singularity spectrum. This can be confirmed by superimposing the singularity spectra of both modes. Thus, both modes exhibit complex behavior.

The examples given indicate different manifestations of the synchronization effect in the multifractal structure of chaotic attractors of coupled systems with self-sustained oscillations, which can be diagnosed using the proposed approach. The aim of this work is to generalize the wavelet-transform modulus-maxima method to the case of cooperative dynamics of complex systems. The presented examples are illustrations confirming the applicability of the proposed approach to solving such problems. We believe that the method can find wider application in studies of cooperative dynamics of various systems, including complex networks.

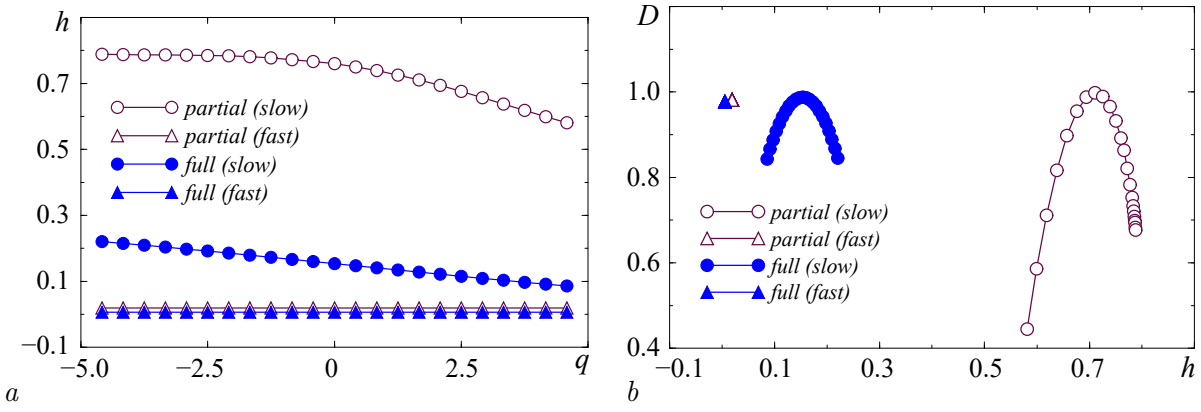

Fig. 5. Multifractal analysis of full and partial synchronization in the model of paired nephrons: *a* — Hölder exponents, *b* — singularity spectra

Conclusion

A generalization of the wavelet-transform modulus maxima method is proposed for the case of cooperative dynamics of systems with self-sustained oscillations. Changes in the joint singularity spectrum during synchronization of chaotic oscillations in the model of coupled Rössler systems are established, which include a change in the type of correlations in the sequences of return times (transition from positive correlations to anticorrelations) and a significant decrease in the width of the spectrum. This allows us to talk about simplifying the dynamics with respect to the number of characteristics necessary for the diagnosis of the mode. When considering partial synchronization in the model of paired nephrons, changes in the position of the joint singularity spectrum are noted, which are associated with the average value of the Hölder exponents (transition to anticorrelations during synchronization of slow oscillations), but are not accompanied by a decrease in the width of the spectrum. The results obtained allow us to conclude that it is possible to diagnose changes in the multifractal structure of chaotic attractors during synchronization of chaos. The proposed generalization of the wavelet-based multifractal formalism can find application in solving a wide range of problems of analyzing the cooperative dynamics of complex systems based on experimental data.

References

1. Bendat JS, Piersol AG. Random Data: Analysis and Measurement Procedures. 4th edition. New Jersey: John Wiley & Sons; 2010. 640 p. DOI: 10.1002/9781118032428.
2. Press WH, Teukolsky SA, Vetterling WT, Flannery BP. Numerical Recipes: The Art of Scientific Computing. 3rd edition. Cambridge: Cambridge University Press; 2007. 1256 p.
3. Halsey TC, Jensen MH, Kadanoff LP, Procaccia I, Shraiman BI. Fractal measures and their singularities: The characterization of strange sets. Phys. Rev. A. 1986;33(2):1141–1151. DOI: 10.1103/PhysRevA.33.1141.
4. Frish U, Parisi G. On the singularity structure of fully developed turbulence. In: Ghil M, Benzi R, Parisi G, editors. Turbulence and Predictability in Geophysical Fluid Dynamics and Climate Dynamics. New York: North-Holland; 1985. P. 84–88.
5. Benzi R, Vulpiani A. Multifractal approach to fully developed turbulence. Rendiconti Lincei. Scienze Fisiche e Naturali. 2022;33(3):471–477. DOI: 10.1007/s12210-022-01078-5.
6. Muzy JF, Bacry E, Arneodo A. Wavelets and multifractal formalism for singular signals: Application to turbulence data. Phys. Rev. Lett. 1991;67(25):3515–3518. DOI: 10.1103/PhysRevLett.67.3515.
7. Muzy JF, Bacry E, Arneodo A. The multifractal formalism revisited with wavelets. International Journal of Bifurcation and Chaos. 1994;4(2):245–302. DOI: 10.1142/S0218127494000204.
8. Kantelhardt JW, Zschiegner SA, Koscielny-Bunde E, Havlin S, Bunde A, Stanley HE. Multifractal detrended fluctuation analysis of nonstationary time series. Physica A: Statistical Mechanics and its Applications. 2002;316(1–4):87–114. DOI: 10.1016/S0378-4371(02)01383-3.
9. Ihlen EAF. Introduction to multifractal detrended fluctuation analysis in Matlab. Frontiers in Physiology. 2012;3:141. DOI: 10.3389/fphys.2012.00141.
10. Meneveau C, Sreenivasan KR, Kailasnath P, Fan MS. Joint multifractal measures: Theory and applications to turbulence. Phys. Rev. A. 1990;41(2):894–913. DOI: 10.1103/PhysRevA.41.894.
11. Ivanov PC, Amaral LAN, Goldberger AL, Havlin S, Rosenblum MG, Struzik ZR, Stanley HE. Multifractality in human heartbeat dynamics. Nature. 1999;399(6735):461–465. DOI: 10.1038/20924.
12. Pavlov AN, Sosnovtseva OV, Ziganshin AR, Holstein-Rathlou NH, Mosekilde E. Multiscality in the dynamics of coupled chaotic systems. Physica A: Statistical Mechanics and its Applications. 2002;316(1–4):233–249. DOI: 10.1016/S0378-4371(02)01202-5.

13. Pavlov AN, Pavlova ON, Abdurashitov AS, Sindeeva OA, Semyachkina-Glushkovskaya OV, Kurths J. Characterizing scaling properties of complex signals with missed data segments using the multifractal analysis. Chaos. 2018;28(1):013124. DOI: 10.1063/1.5009438.
14. Addison PS. The Illustrated Wavelet Transform Handbook: Introductory Theory and Applications in Science, Engineering, Medicine and Finance. 2nd edition. Boca Raton: CRC Press; 2016. 464 p. DOI: 10.1201/9781315372556.
15. Barfred M, Mosekilde E, Holstein-Rathlou NH. Bifurcation analysis of nephron pressure and flow regulation. Chaos. 1996;6(3):280–287. DOI: 10.1063/1.166175.
16. Postnov DE, Sosnovtseva OV, Mosekilde E, Holstein-Rathlou NH. Cooperative phase dynamics in coupled nephrons. International Journal of Modern Physics B. 2001;15(23): 3079–3098. DOI: 10.1142/S0217979201007233.
17. Sosnovtseva OV, Pavlov AN, Mosekilde E, Yip KP, Holstein-Rathlou NH, Marsh DJ. Synchronization among mechanisms of renal autoregulation is reduced in hypertensive rats. Am. J. Physiol. Renal. Physiol. 2007;293(5):F1545–F1555. DOI: 10.1152/ajprenal.00054.2007.